Food Hydrocolloids 146 (2024) 109248

Contents lists available at ScienceDirect

Food Hydrocolloids

journal homepage: www.elsevier.com/locate/foodhyd

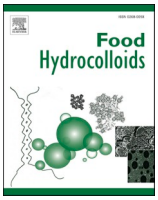

Interfacial moduli at large strains and stability of emulsions stabilised by plant proteins at high bulk shear rates

Naoya Ikenaga [a,b,c], Leonard M.C. Sagis [a,*]

[a] Laboratory of Physics and Physical Chemistry of Foods, Bornse Weilanden 9, 6708 WG, Wageningen, the Netherlands
[b] Fuji Oil Global Innovation Center Europe, Bronland 10, 6708 WH, Wageningen, the Netherlands
[c] Fuji Oil Co., Ltd., 1 Sumiyoshi-cho, Izumisano-shi, Osaka, 598-8540, Japan

ARTICLE INFO

Keywords:
Potato protein
Soy protein
Pea protein
Interfacial rheology
High shear
Emulsion stability

ABSTRACT

For several commercial plant-protein stabilisers, we investigated how surface shear and dilatational properties affect dynamic emulsion stability under high bulk shear conditions. Potato protein isolates Potato-1 (rich in patatin) and Potato-2 (rich in protease inhibitors) showed a stiffer, more solid-like response than soy and pea protein isolates in large amplitude oscillatory surface shear. Soy protein isolates had the weakest interfaces and showed a more liquid-like behaviour. Potato-2 had the highest stiffness and most brittle interface in large amplitude oscillatory dilatational deformations. It also showed more significant softening, evident from both the shear and dilatational Lissajous plots. Only the Potato-1-stabilised emulsion was stable against coalescence at high bulk shear (although that emulsion was unstable against flocculation because of its low zeta potential). The low stiffness imparted to the interface by the pea and soy protein isolates was not suitable for preparing emulsions with high dynamic stability. In the linear regime, both Potato-1 and Potato-2 produced interfaces with similar surface shear moduli, and in dilatation, Potato-2 gave a higher modulus. The lower stability of the Potato-2 emulsions appears to be linked to the higher brittleness and stronger softening effect for increasing deformation amplitude. Both in surface shear and dilatation, the maximum linear strain for the Potato-1-stabilised interface is larger. The lower maximum linear strain and stronger softening effect at high deformations for Potato-2 may have resulted in more disruption of the interfacial microstructure, and this induced (partial) coalescence.

1. Introduction

Sustainability aspects have become an important driver for the development of food products. One way to improve sustainability of food products is by replacing dairy- and meat-based proteins by plant-based proteins (Akharume, Aluko, & Adedeji, 2021; Cornet et al., 2022; Mäkinen, Wanhalinna, Zannini, & Arendt, 2016; Mefleh, Pasqualone, Caponio, & Faccia, 2022; Munekata et al., 2020; Singh et al., 2021). Examples of such products are plant-based dairy drinks. These products are emulsions, with small oil droplets dispersed in a continuous phase containing proteins, salts, and carbohydrates. The added plant protein has a nutritional function but is often also added to stabilise the emulsion against aggregation, coalescence, and creaming. The stability of plant protein-stabilised emulsions, has been studied by measuring the particle size distribution as a function of time, by determining the creaming rate under centrifugation, and by establishing heat resilience for post-processing (Liang & Tang, 2014; McClements, Lu, & Grossmann, 2022; Sridharan, Meinders, Bitter, & Nikiforidis, 2020; Yang, de Wit, et al., 2021). The stability of emulsions is often related to interfacial properties of the oil-water interface, such as its charge, or its mechanical properties like the surface shear or dilatational modulus. These properties have also been studied widely in recent years (Braun, Hanewald, & Vilgis, 2019; Hinderink, Sagis, Schroën, & Berton-Carabin, 2021; McClements et al., 2022; Ntone et al., 2021). But stability of plant-based emulsions is mostly assessed under quiescent conditions, and their behaviour under high shear conditions, highly relevant for their processing, has not been well studied.

This is also true for applications of plant protein-stabilised emulsions in other types of products, such as meat replacers, processed in extruders. In these products emulsions are added to control juiciness or as a carrier for flavours. In the extruder, the emulsions are exposed to high deformation rates, which can disrupt the interfacial films stabilising the droplets, resulting in coalescence. The addition of oil to these products during extrusion can have a significant effect on their texture (Kendler,

* Corresponding author.
E-mail address: leonard.sagis@wur.nl (L.M.C. Sagis).

https://doi.org/10.1016/j.foodhyd.2023.109248
Received 15 May 2023; Received in revised form 11 August 2023; Accepted 30 August 2023
Available online 30 August 2023

Duchardt, Karbstein, & Emin, 2021; Osen, Toelstede, Wild, Eisner, & Schweiggert-Weisz, 2014; Wang et al., 2022; Zhang, Liu, Jiang, Faisal, & Wang, 2020).

This study aims to explore the suitability of commercially available potato, soy, and pea protein isolates for stabilising emulsions in plant-based dairy drinks. We have chosen commercially available stabilisers here since most manufacturers do not use highly purified plant protein extracts in the production of emulsion-based products. We have characterized these stabilisers with respect to composition, particle size distribution, and average molecular weight. The interfacial properties of oil-water interfaces stabilised by these samples were studied using Small and Large Amplitude Oscillatory Shear (SAOS and LAOS) and Small and Large Amplitude Oscillatory Dilatation (SAOD and LAOD). The shear and dilatational storage and loss modulus were determined, and the nonlinear behaviour was analysed using Lissajous plots. Emulsions were prepared and subsequently characterized by measuring their size distribution and zeta-potential. The dynamic stability of the oil-water emulsions was tested by applying high shear using an Ultra Turrax blending device and again determining the droplet size distribution using light scattering. The results obtained here can facilitate the development of stable plant-based dairy drinks. The results may also have ramifications for the production of meat replacers.

2. Materials and methods

2.1. Materials

Medium-chain triglyceride (MCT) oil (MIGLYOL® 812N) was purchased from IOI Oleochemical (France). Commercial potato protein isolates (PoPI), Potato-1 and Potato-2) were kindly donated by Avebe U. A. (Netherlands). Commercial soy protein isolates (SPI), Soy-1, Soy-2, Soy-3, and Soy-4 were kindly donated by Fuji Oil Co., Ltd. (Japan). A commercial pea protein isolate (PePI), Pea-1, was purchased from Roquette Frères (France). Details on protein content, average molecular weight, and processing of the isolates are given in Table 1, and composition, and number mean particle size of these protein isolates are shown in Tables S1 and S2. Milli-Q water (PURELAB® Ultra Water Purification System, Germany) was used for all experiments. Florisil® (60–100 mesh), sodium azide, hydrochloric acid (HCl), sodium hydroxide (NaOH), and sodium chloride (NaCl) were purchased from Merck (Germany).

2.2. Methods

2.2.1. Sample preparation

2.2.1.1. Purification of MCT oil. Florisil was dried overnight in an oven at 120 °C, then cooled to room temperature in a desiccator. MCT oil was mixed with 10 wt% Florisil and stirred at 20 °C. Samples of MCT oil were taken every hour, and filtered using a syringe filter to remove Florisil, followed by measurement of the interfacial tension of the MCT oil - Milli-Q water interface, until the tension became constant. Then, MCT oil was centrifuged at 4500×*g* for 10 min to remove Florisil, and the supernatant was filtered using filter paper (Whatman, Grade 4, diam.90 mm, England). Purified MCT oil was stored in a glass bottle in a dark place at 20 °C until used.

Table 1
Details of the protein isolates. Protein content was measured by Dumas method (see Sec 2.2.1.2), and weight average molecular weight was obtained using HPLC.

Supplier	Source	Protein name	Processing by supplier	pH	Protein content (wt%)	M_w (kDa)
Avebe	Potato	Potato-1	Extracted from potato protein	Neutral	77.18	80
		Potato-2	Extracted from potato protein	Acidic	77.67	32
Roquette	Pea	Pea-1		Neutral	69.36	94
Fuji Oil	Soy	Soy-1		Neutral	75.64	140
		Soy-2	Hydrolysed	Neutral	74.86	118
		Soy-3	Hydrolysed	Neutral	74.96	51
		Soy-4		Neutral	76.90	167

2.2.1.2. Protein dispersions. The protein content of all protein powders was determined by Dumas. A nitrogen conversion factor of 5.5 was used as an average for all proteins for convenience (Mariotti, Tomé, & Mirand, 2008). Based on Dumas results, all powders were dispersed in Milli-Q water at a concentration slightly higher than 1.76 wt%, which is enough to stabilise a 10% oil-in-water emulsion as described by Yang, de Wit, et al. (2021); 0.02 wt% sodium azide was added to all dispersions. The dispersions were stirred at 20 °C for 4 h, then at 4 °C for 20 h. The pH and conductivity of the dispersions were adjusted using 1.0 M HCl, 1.0 M NaOH, and NaCl to pH 3.6 for Potato-2 (which has an acidic pH in water) and pH 7.0 for all others, and 1300 μS/cm. After that, the protein dispersions were diluted with pH- and conductivity-adjusted water (pH 3.6/7.0 and 1300 μS/cm) to 0.044, 0.22, 0.44, 0.88, and 1.76 wt%.

2.2.1.3. Emulsion preparation. Emulsions with 10% MCT oil content were prepared with the protein dispersions. The mixtures were first pre-homogenised using an ULTRA-TURRAX® (IKA T25, Germany) with S25N-18G dispersing tool at 5000 rpm for 5 min. Then, the pre-homogenised mixture was homogenised by a high-pressure homogeniser (LAB, Delta Instruments, The Netherlands) at 150 bar for 10 passes (to make the particle size distribution as narrow as possible) at room temperature. The beaker for collecting the emulsions was in ice water during homogenisation to prevent excessive heating. The emulsions were finally collected in a blue cap bottle and stored overnight at 4 °C before analysis.

2.2.2. Interfacial shear properties

Interfacial shear properties of oil-water interfaces stabilised by the plant protein isolates were studied using a magnetic bearing rheometer (AR-G2, TA Instruments, USA) with a double-wall-ring (DWR) geometry, as described by Yang, Faber, et al. (2021). The protein dispersion was poured into a double wall cylindrical trough. After the ring was positioned at the air-dispersion interface, the purified MCT oil was carefully poured on top of the protein dispersion without disturbing it. Before all measurements, a pre-shear was applied to the sample at a shear rate of 10 1/s for 5 min. Time sweeps were performed at a strain of 1.0% and a frequency of 1.0 Hz for 10800 s. Subsequently, frequency sweeps were performed at a strain of 1.0% with frequencies ranging from 0.01 Hz to 10.0 Hz, followed by strain sweeps at a frequency of 1.0 Hz with strains ranging from 0.1% to 100%. All measurements were performed at 20 °C.

2.2.3. Interfacial dilatational properties

Interfacial dilatational properties of oil-water interfaces stabilised by plant proteins were determined using a TRACKER™ Automatic Drop Tensiometer & Dilatational Interfacial Rheometer (ADT) (Teclis, France) as described by Zhou, Sala, and Sagis (2020). A protein dispersion of 0.044 wt% was poured into a cuvette. A curved needle connected to a motor driven syringe (Trajan Scientific and Medical, Australia) was submerged in the solution. A rising droplet of purified MCT oil with a surface area of 30 mm^2 was created. After monitoring the interfacial tension for 2–3 h, amplitude and frequency sweeps were performed by applying sinusoidal oscillatory area deformations for five cycles, followed by 900 s recovery time for each condition. The amplitude sweeps were run at a frequency of 0.02 Hz with amplitudes ranging from 5% to

20%. Frequency sweeps were run at an amplitude of 5% with frequencies ranging from 0.005 Hz to 0.05 Hz. Before each sweep, the oil droplet was released, and a new one was made at the tip of the needle. The oscillations of all measurements were performed at 20 °C. Note that we did not oscillate during the adsorption phase of the protein. Monitoring the development of the dilatational modulus in a time sweep, as we did for the surface shear measurements, is possible only when the measurement can be performed in the linear viscoelastic regime. At the smallest deformation amplitude, we can apply with the tensiometer and still get reliable results, we are already in the nonlinear regime. Oscillations would hence affect the structure during its formation.

2.2.4. Lissajous plot analysis

The nonlinear responses in the strain sweeps in both surface shear and dilatational mode were analysed by making Lissajous plots. The plots prepared from the data of the interfacial shear measurements were automatically generated using the Trios software of the AR-G2, plotting the time dependent torque signal versus strain. The time dependent surface tension data from the dilatational measurements was converted into surface pressure ($\pi(t) = \sigma(t) - \sigma_0$) and plotted against the deformation ($(A(t) - A_0)/A_0$). as described by Rühs, Scheuble, Windhab, and Fischer (2013); Sagis and Fischer (2014). Here, σ and A are the surface tension and area of the interface of the oil droplet, and subscript "0" indicates values of these for the non-deformed interface. The middle three of the five cycles were used for creating the plots.

2.2.5. Emulsion analysis

2.2.5.1. Zeta potential. The zeta potential of the protein-stabilised oil droplets in the emulsions was measured with a Zetasizer Ultra (Malvern Panalytical, UK). The emulsions were diluted 200 times with pH- and conductivity-adjusted water (pH 3.6/7.0 and 1300 μS/cm). Each measurement was run five times at 20 °C, and those results were averaged. A refractive index of 1.45 and absorption index of 0.001 were used for the dispersed phase. For the dispersant, 1.33 was used as the refractive index. The diluted samples were measured in a DTS1070 cell.

2.2.5.2. Particle size distribution. The particle size distribution of the emulsions was measured using a Mastersizer 2000 (Malvern Panalytical, UK). Measurements were performed before application of high shear (0 min) and after different duration of shear (5, 10, and 15 min). Each measurement was run twice, and those results were averaged. For MCT oil, refractive and absorption indices of 1.45 and 0.001 were used, respectively. For the dispersant, 1.33 was used as the refractive index.

2.2.5.3. Stability of the emulsions against high shear rates. The emulsions were put in ice water and subjected to high shear using an ULTRA-TURRAX® (IKA T25, Germany) with an S25N-10G dispersing tool at 13000 rpm. Samples for the particle size distribution measurement were taken after 5, 10, and 15 min of shearing.

3. Results and discussion

3.1. Small and large amplitude oscillatory shear (SAOS and LAOS)

3.1.1. Time sweep

To study the surface shear rheology of the plant protein-stabilised interfaces between oil and water, small amplitude oscillatory shear (SAOS) was performed. In the 3-h time sweep, Potato-1 and Potato-2 (Fig. 1A&B) showed a higher G′ than G″ from the first data point from the start of the time sweep, suggesting the proteins in these isolates adsorbed at the interface and quickly formed viscoelastic solid-like structures. This high rate of adsorption could be due to the small average size of these proteins (roughly 8 nm for Potato-1 and 4 nm for Potato-2; see Table S2). Pea-1 (Fig. 1C) initially showed a lower G′ than G″, until a crossover occurred at about 20 s, after which G′ was higher than G". Structure formation was clearly slower for this component compared to Potato-1 and Potato-2. The G′ values were also significantly lower for Pea-1 (~20 mN/m) compared to Potato-1 and Potato-2 (100–200 mN/m), and the latter two clearly produce stiffer interfaces. All SPIs (Soy-1, Soy-2, Soy-3, and Soy-4) showed similar results, producing very weak structures on the interface with predominantly viscous behaviour (In Fig. 1D we show results only for Soy-1). The G' values for the SPIs were very low (<1 mN/m) and difficult to measure accurately. These observations suggest that in-plane interactions between proteins are stronger in the Potato-1 and Potato-2 samples.

3.1.2. Frequency sweeps

After the time sweep, frequency sweeps (Fig. 2) were applied to the interfaces stabilised by Potato-1, Potato-2, and Pea-1 (Fig. 2A–C). All three showed a higher G′ than G″ for the entire range of applied frequencies, and displayed a weak power-law dependence on frequency

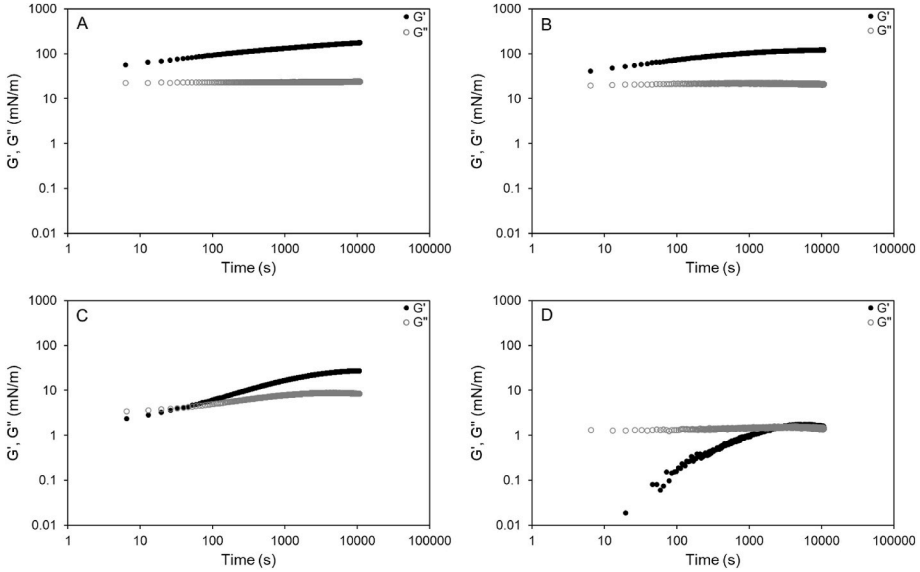

Fig. 1. G' (closed symbols) and G" (open symbols) versus time of oil-water interfaces stabilised by (A) Potato-1, (B) Potato-2, (C) Pea-1 and (D) Soy-1 in surface shear at 1% strain and 1 Hz frequency. For clarity, one representative result is shown, but comparable results were obtained for two replicates.

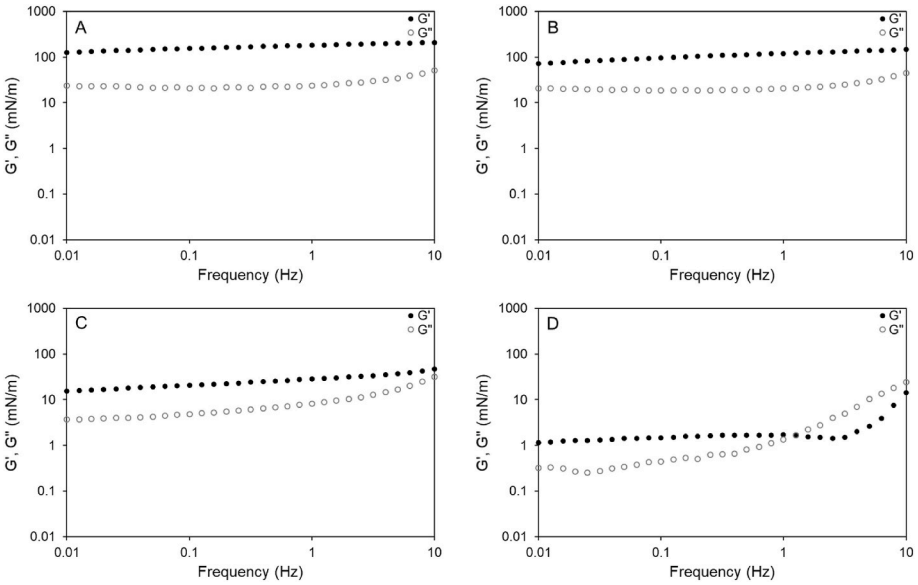

Fig. 2. G' (closed symbols) and G" (open symbols) as a function of the frequency of the oil-water interfaces stabilised by (A) Potato-1, (B) Potato-2, (C) Pea-1, and (D) Soy-1 in surface shear at 1% strain. For clarity, one representative result is shown, but comparable results were obtained for two replicates.

(G'~f^n) with low n-values (~0.2), which is commonly observed for disordered solids such as gels or soft glassy systems (Winter & Mours, 1997) and proteins such as β-lactoglobulin (Cicuta, Stancik, & Fuller, 2003). This weak frequency dependence was also observed for interfaces stabilised by whey, rapeseed, BSA and Acacia gum (Erni et al., 2007; Jaishankar & McKinley, 2013; Yang, Faber, et al., 2021; Yang, Thielen, Berton-Carabin, van der Linden, & Sagis, 2020). These results suggest that Potato-1, Potato-2 and Pea-1 formed a soft solid-like structure after adsorption at the interface. For the interfaces stabilised by Soy-1 (Fig. 2D), Soy-2, Soy-3, and Soy-4, an upswing in G' and G″ at frequencies above 1 Hz was observed (only Soy-1 data is shown). This upswing most likely resulted from inertia effects, typically happening in a weak and mobile interface (Delgado et al., 2018; Ewoldt, Johnston, & Caretta, 2015; Läuger & Stettin, 2016).

3.1.3. Strain sweeps

Strain sweeps were also performed on the interface stabilised by Potato-1, Potato-2, and Pea-1 (Fig. 3A–C). The response of Potato-1- and Potato-2-stabilised interfaces was dominated by elasticity up to a strain of 3.2% and 2.0%, respectively. Beyond this strain, G′ was smoothly decaying, indicating a gradual disruption of the interfacial microstructure. A weak strain overshoot (Payne effect) in G″ of Potato-1 and Potato-2 was also observed, followed by a gradual decrease. The maximum in G″ coincides with the crossover point, beyond which G"$>$G', and the response of the material becomes progressively dominated by viscosity rather than elasticity. This type of behaviour is often referred to as Type III nonlinear behaviour (Hyun, Kim, Ahn, & Lee, 2002). In the regime of the overshoot, the rate of network bond disruption is slower than the rate of new bond formation, leading to a slight increase in G" (Hyun et al., 2002). Donley, Singh, Shetty, and Rogers (2020) recently showed that the overshoot is associated with a yielding transition from linear

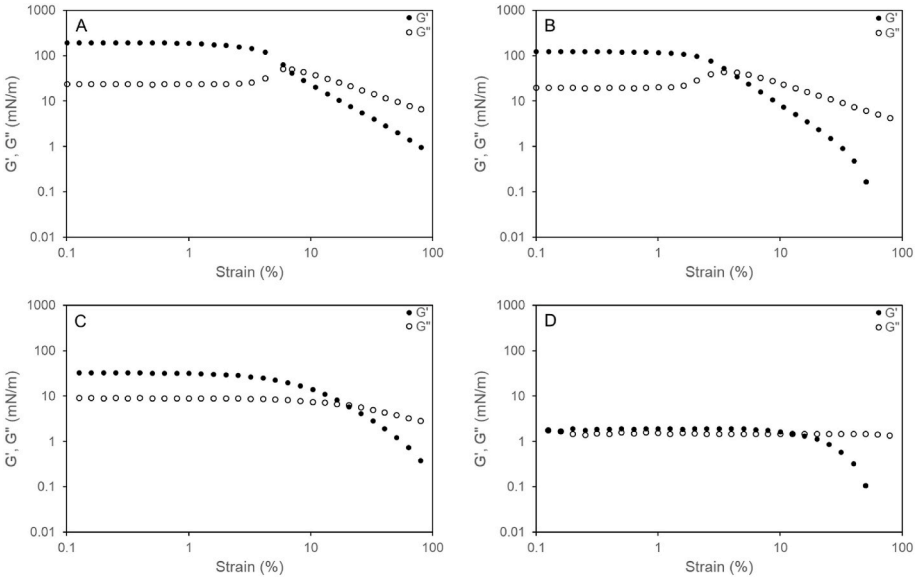

Fig. 3. G' (closed symbols) and G" (open symbols) as a function of the strain of the oil-water interfaces stabilised by (A) Potato-1, (B) Potato-2, (C) Pea-1 and (D) Soy-1 in shear at 1 Hz frequency; again, only one representative result is shown, but comparable results were obtained for two replicates.

solid-like viscoelastic behaviour to primarily fluid-like plastic flow. A similar weak overshoot was observed for the air-water interface stabilised by whey protein isolate (Yang, Waardenburg, et al., 2021). The Pea-1-stabilised interface showed lower G′ and G″ than Potato-1 and Potato-2 in the linear region, and its tanδ was much closer to 1. This component did not show an overshoot in G", and both moduli were decreasing smoothly with increasing strain. This strain softening behaviour is sometimes referred to as Type I nonlinear behaviour (Hyun et al., 2002). This result suggests that for Pea-1, the in-plane interactions between proteins were weaker, and its interface was therefore less stiff than the interface stabilised by Potato-1 and Potato-2. The interfaces stabilised by Soy-1 (Fig. 3D), Soy-2, Soy-3, and Soy-4 proved to be too weak to obtain reliable LAOS data, and their results were poorly reproducible. Since their tanδ was almost one and G′ and G″ were low, their interfaces may be considered to be in a liquid-like state.

3.1.4. Lissajous plots of LAOS

The results of the strain sweeps were also analysed by making Lissajous plots of stress versus strain (Ewoldt, Hosoi, & Mckinley, 2008; Rühs et al., 2013). The values for G' and G" are based on a Fourier Transform of the stress signal and calculated from the intensity and phase of the first harmonic of the spectrum. Contributions from higher odd harmonics, which are present in the nonlinear viscoelastic regime, are not accounted for in the calculation. Lissajous plots analyse the full nonlinear stress response, and this can provide additional insights on the microstructure and mechanical properties of oil-water interfaces stabilised food and non-food materials (García-Moreno et al., 2021; Hong et al., 2019; Kieserling et al., 2021). In the linear region, Potato-1- and Potato-2-stabilised interfaces had Lissajous plots with a narrow ellipsoidal shape, suggesting that the responses of those interfaces were dominated by the elastic contribution to the total stress (Fig. 4). When the strain was larger than 3.2% for Potato-1 and 2% for Potato-2, the plots became wider, and quickly transitioned to a rhomboidal shape, indicative of yielding of the interfacial structure, and a transition to plastic behaviour. On the other hand, the Pea-1-stabilised interface showed relatively wider Lissajous plots even at a low strain, indicative of a relatively higher viscous contribution to the stress. The transition to liquid-like behaviour is also more gradual than for Potato-1 and Potato-2. The interfaces stabilised by Soy-1, Soy-2, Soy-3, and Soy-4 were too weak to measure accurately and showed visco-inertial behaviour (Fardin et al., 2014) in the Lissajous curves, evident from the negative slope the main axis of the plot has with respect to the vertical axis. In Table S2 we see that Potato-1 and Potato-2 are likely in a monomeric state. Pea-1 has an average size of about 40 nm, indicating that a significant fraction of these proteins is present in an aggregated state. The Soy proteins have the largest particle size (in a range of 30–100 nm). It is likely that because of their smaller size Potato-1 and Potato-2 were able to form denser and more homogeneous interfacial layers, with stonger in-plane interactions, resulting in higher stiffness and a more elastic behaviour at small strains. In Pea-1 and the soy samples, the in-plane interactions were clearly much weaker. This will also become more evident, when analyzing the dilatational response of the interfaces.

3.2. Small and large amplitude oscillatory dilatation (SAOD and LAOD)

3.2.1. Frequency sweeps

The plant protein-stabilised oil-water interfaces were also subjected to small amplitude oscillatory dilatation (frequency sweeps) and large amplitude oscillatory dilatation (LAOD). Fig. 5A–B shows the elastic dilatational modulus (Ed') and viscous dilatational modulus (Ed") as a function of the frequency in the linear regime. Clearly, Ed' was higher than Ed" for all protein-stabilised interfaces, and all interfaces showed a power law behaviour ($Ed' \sim f^n$), in agreement with the observations in LAOS. The scaling exponent (n) of Potato-2 was the highest of all proteins at a value 0.09; this is significantly lower than the value of 0.5 predicted by the Lucassen & Van Den Tempel model (Lucassen & Van Den Tempel, 1972). This implies that contributions to dissipation resulting from diffusion from the bulk to the interface were negligible for all protein isolates, on the timescales we are considering here. This weak frequency dependency behaviour in dilatation was also observed on the interfaces stabilised by whey protein isolate and proteins from silkworm pupae (Felix, Yang, Guerrero, & Sagis, 2019), and is consistent with the frequency response in the SAOS measurements.

3.2.2. Amplitude sweeps

In the amplitude sweeps, the elastic moduli of Potato-1- and Potato-2-stabilised interfaces decreased with increasing amplitude from 20.0 mN/m to 15.1 mN/m and 27.8 mN/m to 19.6 mN/m, respectively. This result indicated that some interactions between protein clusters started to break at a larger amplitude. The Potato-2-stabilised interfaces had a similar amplitude dependence to a whey protein isolate-stabilised oil-water interface (Hinderink, Sagis, Schroën, & Berton-Carabin, 2020). Pea-1-, Soy-1-, Soy-2-, Soy-3-, and Soy-4-stabilised interfaces showed a weak amplitude dependence of their elastic moduli, suggesting that their structures on the interface had weak in-plane interactions, in agreement with the LAOS results.

3.2.3. Lissajous plots

To further characterise these interfaces, the data was analysed by making Lissajous plots of surface pressure versus deformation as described by (Fig. 7). The Potato-2-stabilised interface (Fig. 7B) showed

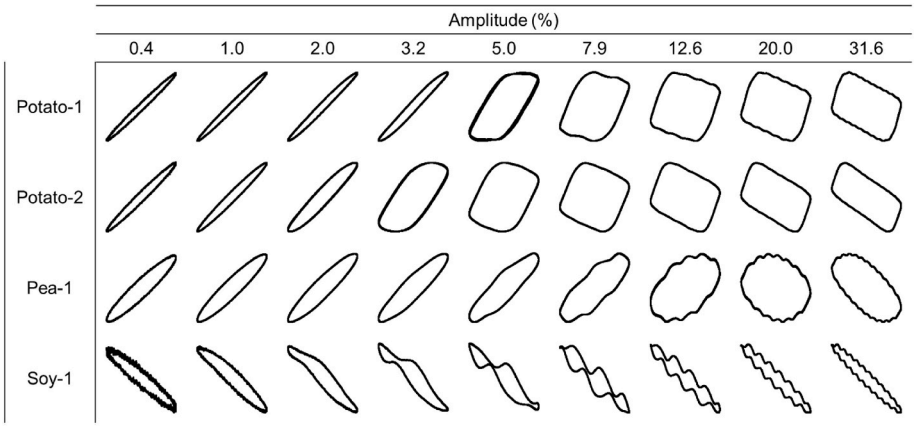

Fig. 4. Lissajous plots of torque as a function of the strain for the strain sweeps of Fig. 3. All plots were normalised using their maximum value for torque and strain. One representative result for Potato-1, Potato-2, and Pea-1 is shown, but comparable results were obtained on two replicates. For Soy-1, Soy-2, Soy-3, and Soy-4, only one measurement was performed since their interfaces were too weak to measure accurately. Only Soy-1's data is shown.

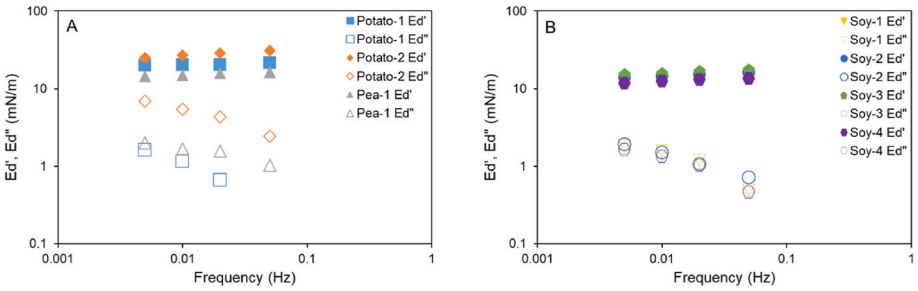

Fig. 5. Ed' (closed symbols) and Ed" (open symbols) as a function of frequency of oil-water interfaces stabilised by plant proteins in dilatation at 5% amplitude. For clarity, one representative result for (A) Potato-1, Potato-2, and Pea-1 and (B) Soy-1, Soy-2, Soy-3, and Soy-4 is shown, but comparable results were obtained for two replicates.

the stiffest behaviour since its Lissajous plots were the steepest among all protein-stabilised interfaces. It also formed the most brittle interface and showed significant softening in expansion, suggested by the slope change from steep in compression to nearly horizontal in expansion, especially at the larger deformations (15 and 20%). The other protein-stabilised interfaces showed more stretchable and less brittle behaviour. Among these stretchable interfaces, the Potato-1's interface had a bit stiffer structure since the slope of the plot was steeper than the others. The near linear behaviour and low value for the stiffness for the Soy stabilised interfaces confirms our earlier hypothesis based on the LAOS results that the in-plane interactions between the proteins are weak, and these interfaces have mostly liquid-like behaviour. The narrow shape of the plots, combined with the low value for the dilatational loss tangent observed in Fig. 6, would suggest elastic behaviour. But for these components the main dissipative mechanism is likely to be diffusive exchange between bulk and interface, and on the timescale of our deformations, diffusion appears to be too slow to compensate for changes in surface density caused by compression/extension. The dilatational Lissajous plots for Potato-2 were wider than those of the other samples and show a much more significant softening when the amplitude is increased. This is consistent with the results of LAOS in Fig. 4 where the plot of Potato-2 transitioned to a rhomboidal shape at much lower strain and over a shorter strain range. So, the increased stiffness and brittleness we observed in surface shear is confirmed by the dilatational measurements. Similarly, to what we observed in shear, Potato-1 gives somewhat lower stiffness, but the changes in the shape of the plots with increasing strain are less pronounced, and the softening of the structure is milder, confirming the higher stretchability of these interfaces.

3.3. Stability of emulsions

To study whether the difference in characteristics of the oil-water interfaces stabilised by these proteins affects the stability of emulsions, the zeta potential was measured, and the emulsions' stability was tested when subjected to high shear, by determining its particle size distribution and using microscopy.

3.3.1. Zeta potential

For each emulsion, the zeta potential at different protein concentrations was measured, at the same conductivity and pH (pH 3.6 for Potato-2 and 7.0 for the others) (Table 2). Only the zeta potential of the Potato-1-stabilised emulsion was less than 20 mV at all protein concentrations in terms of the absolute value of the potential; 20 mV is often assumed to be the minimum value needed to stabilise an emulsion against flocculation by electrostatic and steric stabilisers (Arunkumar, Deecaraman, & Rani, 2009; Riddick, 1968; Schramm, 2005, pp. 117–154). The other proteins' emulsions had a larger absolute value of the zeta potential, suggesting that these emulsions should be stable against flocculation. Note that with increasing protein concentration there is a slight decrease in absolute value of the zeta potential. This was also observed by Phianmongkhol and Varley (2003), for the zeta potential of protein-stabilised air bubbles. These authors speculated that differences in the structuring of water molecules at the interface are responsible for this effect.

3.3.2. Particle size distribution after subjecting to high shear

The particle size distribution of emulsions was measured before and after being subjected to high shear. The emulsions at various protein concentrations were subjected to high shear for 15 min while being cooled with ice water. Only the 1.76% protein concentration data is shown for each protein (Fig. 8) and the D[4, 3] of the emulsions subjected to high shear is given in Table S3. The Potato-1 emulsion (Fig. 8A) had a bimodal distribution prior to shearing with a peak at about 400 nm and a second peak around 8 μm, and the latter disappeared after applying shear for 5 min. This emulsion had a zeta potential of about −10 mV, and this low value most likely induced flocculation. The loosely aggregated flocs broke up as a result of shearing, resulting in the disappearance of the second peak. Increasing the shear time from 5 to 10 or 15 min did not further reduce the average droplet size. The

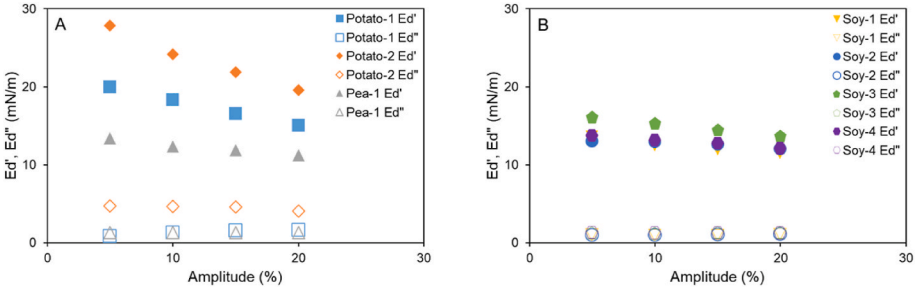

Fig. 6. Ed' (closed symbols) and Ed" (open symbols) as a function of the amplitude of the oil-water interfaces stabilised by plant proteins in dilatation at 0.02 Hz frequency. One representative result for (A) Potato-1, Potato-2, Pea-1 and (B) Soy-1, Soy-2, Soy-3, and Soy-4 is shown, but comparable results were obtained for two replicates.

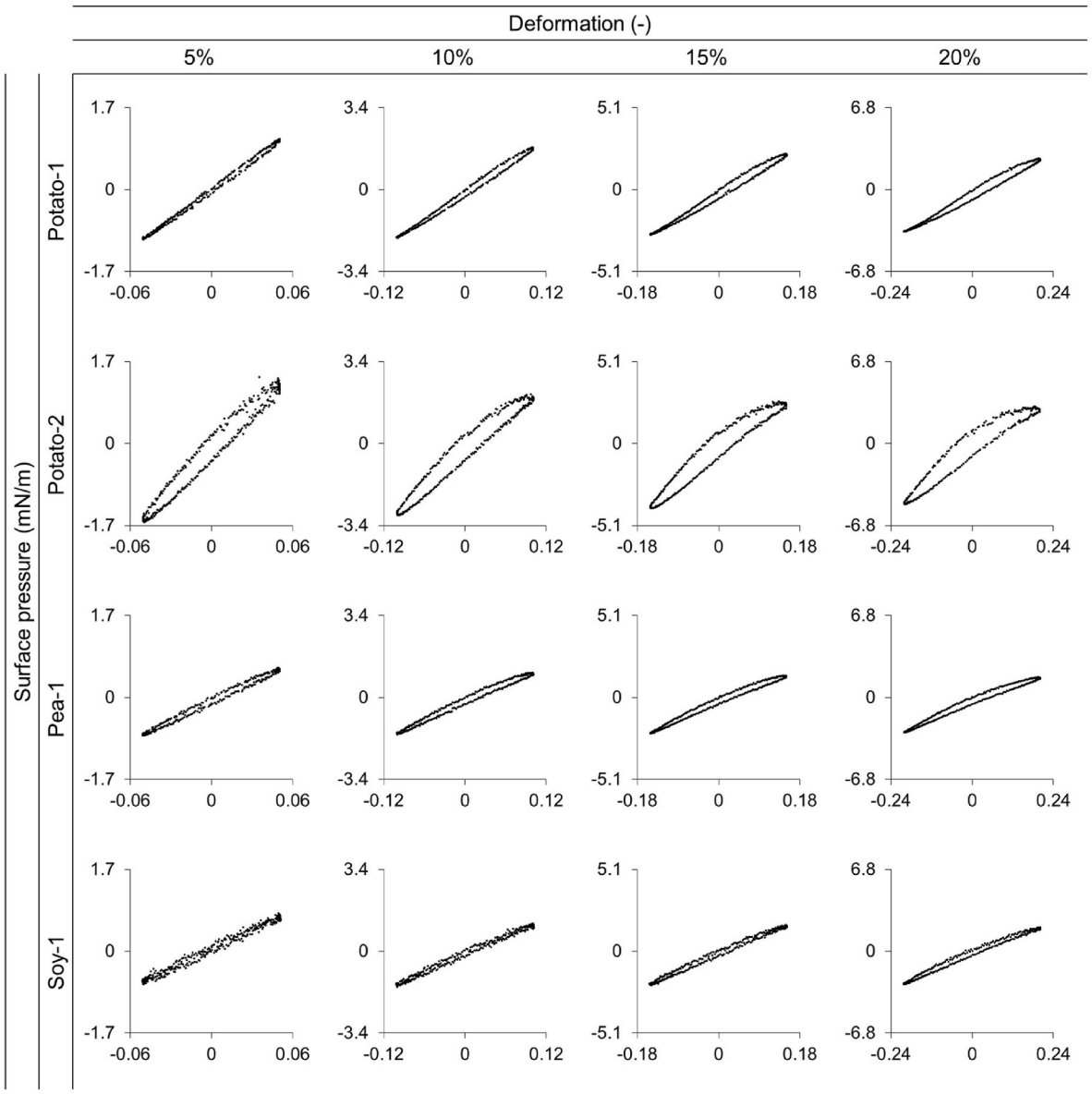

Fig. 7. Lissajous plots of surface pressure versus deformation obtained from the amplitude sweeps (Fig. 6). For each amplitude (5, 10, 15, and 20%) one cycle was plotted for each (Soy-2, Soy-3, and Soy-4 showed similar results to Soy-1 and are not shown).

Table 2
Zeta potential of protein-stabilised emulsions at various protein concentrations. The emulsions were standardised on conductivity (1300 μS/cm) and pH (3.6 for Potato-2 and 7.0 for the others) and were diluted 200 times by water with the same conductivity and pH, prior to measurement. The measurements were repeated five times for each sample, and two replicates were prepared for each emulsion.

Conc. (wt%)	Proteins						
	Potato-1	Potato-2	Pea-1	Soy-1	Soy-2	Soy-3	Soy-4
1.76	−10.41 ± 1.11	37.44 ± 1.71	−22.43 ± 1.96	−26.68 ± 1.07	−24.98 ± 1.78	−28.99 ± 1.55	−25.69 ± 1.55
0.88	−12.03 ± 0.89	42.85 ± 1.49	−24.13 ± 1.72	−26.05 ± 1.39	−28.26 ± 1.20	−29.46 ± 1.75	−27.44 ± 0.82
0.44	−12.31 ± 1.17	46.13 ± 1.26	−25.12 ± 2.03	−29.45 ± 0.76	−32.02 ± 1.29	−34.00 ± 1.96	−29.44 ± 1.24
0.22	−15.09 ± 0.89	47.55 ± 1.36	−26.82 ± 2.01	−32.08 ± 0.91	−30.92 ± 0.85	−34.24 ± 1.48	−30.27 ± 1.52

disappearance of the peak suggests that although the emulsion is not stable against flocculation, it appears to be stable against coalescence, at least on the timescale of this experiment. The Potato-2-, Soy-1-, Soy-2-, and Soy-4-stabilised emulsions (Fig. 8B, D, E, and G) seemed stable against high shear, since their size distribution did not change from the non-sheared one, even after 15 min of shear. In the Pea-1 emulsions (Fig. 8C), a small shoulder was visible around 8 μm and its peak height decreased when the emulsion was subjected to high shear. This again suggests break up of clusters by the applied shear. For the Soy-3-stabilised emulsion, a small shoulder appeared with a peak slightly beyond 10 μm, after 15 min of shearing. This could indicate a minor degree of coalescence occurred, but the effect is very small. Soy-3 has the smallest weight average molecular weight of the four Soy samples and is a hydrolysed SPI (Table 1). This change in molecular size may

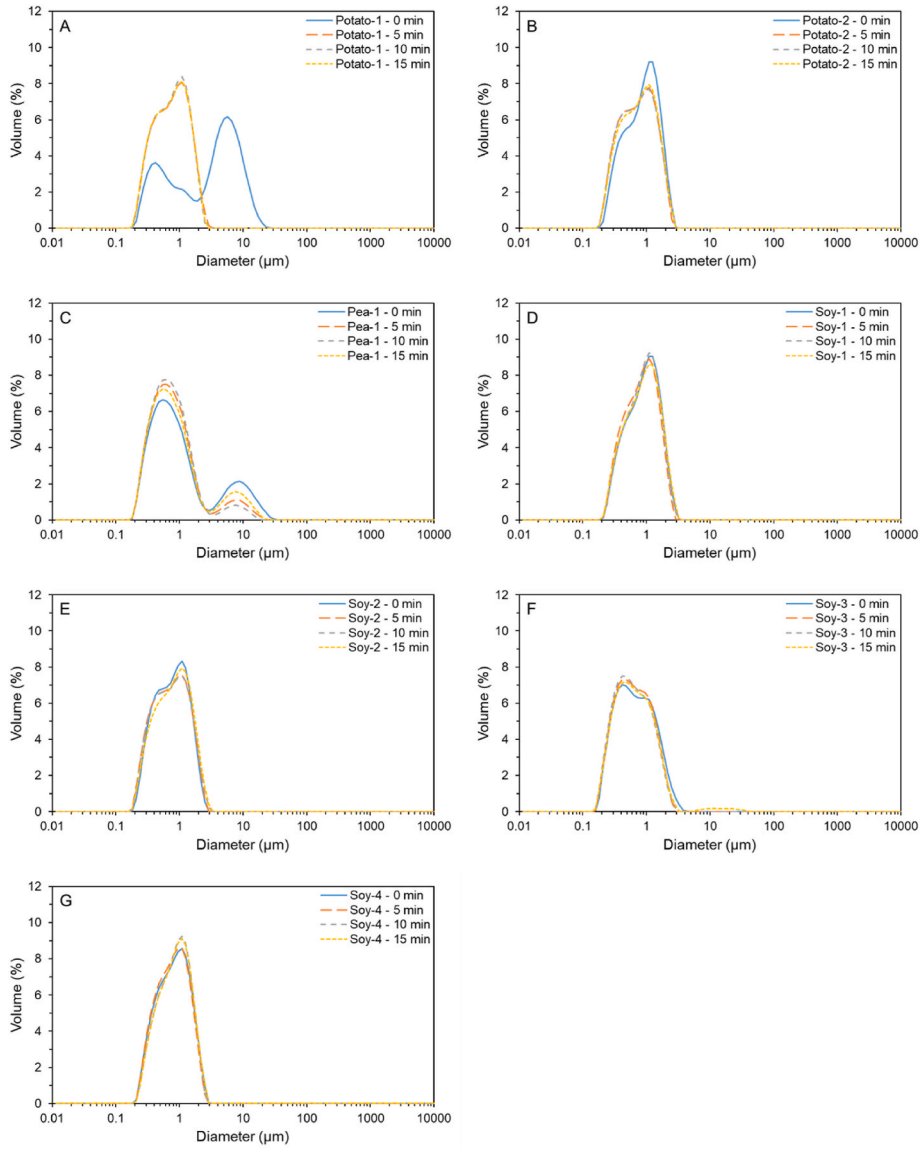

Fig. 8. Particle size distribution of emulsions stabilised by proteins. The distribution was measured before the emulsion was subjected to high shear (0 min) and during the high shear experiment at different times (5, 10, and 15 min). For clarity, one representative result for all emulsions is shown, but comparable results were obtained for two replicates.

affect the stability of the emulsion against shear. This can be due to decreased surface hydrophobicity (Liu, Bhattarai, Mikkonen, & Heinonen, 2019), or weaker in-plane interactions. Optical microscopy was performed to check the results of the droplet size measurements, by taking a small amount of sample at 0 (Fig. S1), 5, 10, and 15 min (Fig. S2). Small flocs of droplets were visible in the Potato-1-stabilised emulsion (Fig. S2A) after 15-min of high shear, although its particle size distribution showed one peak (Fig. 8A). But the droplets themselves did not appear to coalesce even after 15 min of high shear was applied. The fact that we see clusters under the microscope, indicates the droplets started to flocculate again within the time between the moment their particle size was measured, and they were observed with microscopy. In the other emulsions (Figs. S2B–G), many large, coalesced oil droplets were observed. These were not detected by the particle size measurements probably because the number of large droplets was not enough to be detected. The Potato-2-stabilised emulsion had a few oddly shaped (partially) coalesced droplets, probably because of its strong interface, observed in SAOS (Sec 3.1), SAOD, and LAOD (Sec 3.2). So, it appears that although the Potato-1 emulsion was not stable against flocculation, it is the only one that is stable against coalescence in high shear.

4. Conclusions

This study investigated how protein sources affect the mechanical properties of oil-water interfaces for several commercial plant-protein stabilisers, and how these properties affect dynamic emulsion stability under high shear conditions. When protein-stabilised interfaces were subjected to small amplitude oscillatory shear, the potato protein isolates Potato-1 and Potato-2 showed a stiffer, more solid-like response than the soy and pea protein isolates. The soy protein isolates had the weakest interfaces and showed a more liquid-like behaviour in oscillatory shear. Potato-2 appeared to have the stiffest and the most brittle interface in large amplitude oscillatory dilatational deformations. It also had a more significant softening behaviour, as evident from both the shear and dilatational Lissajous plots. When emulsions stabilised by these proteins were subjected to high shear, only Potato-1 appeared to be stable against coalescence (although that emulsion was unstable against flocculation because of its low zeta potential). Apparently, the

low stiffness imparted to the interface by the pea and soy protein isolates is not suitable for preparing emulsions with high dynamic stability. Based on Table 1 and Table S2, hydrolysis does not appear to significantly improve stability of the emulsions stabilised by the SPIs. When examining the protein particle size, Soy-2 and Soy-3 have smaller particle sizes than Soy-1 and Soy-4, but they still have larger particle size than Potato-1 and Potato-2. Hydrolysis can produce a wide range of polypeptides, ranging from hydrophilic, to amphiphilic and hydrophobic peptides; the latter are often poorly water-soluble and tend to aggregate into clusters. When the amphiphilic fraction is small, hydrolysis tends to lead to interfaces with low stiffness and a liquid-like behaviour. Higher degrees of hydrolysis can also result in bitter off-tastes and a lot of free amino acids, for which it is not well-known how they affect the interface under high shear. The difference between Potato-1 and Potato-2 is more subtle. They produced interfaces with similar surface shear moduli, and in dilatation, Potato-2 gave a higher modulus. And yet Potato-1 produced emulsions which were more stable against coalescence. A more important difference appears to be the higher brittleness and stronger softening effect for increasing deformation amplitude for the Potato-2-stabilised interfaces. Both in surface shear and dilatation, the maximum linear strain for the Potato-1-stabilised interface is larger. The lower maximum linear strain and stronger softening effect at high deformations for Potato-2, may have resulted in more disruption of the interfacial microstructure, and this induced (partial) coalescence. In Table 1 we see that Potato-2 has a significantly smaller weight average molecular weight (32 kDa) than Potato-1 (80 kDa). This may have led to a denser and more brittle interfacial structure for Potato-2. There are also compositional differences, where Potato-1 is rich in patatin and Potato-2 rich in protease inhibitors (Tan, Wannasin, & McClements, 2022). Patatin has a low amount of disulfide bonds and high amount of exposed hydrophobic amino acids (Andlinger, Röscheisen, Hengst, & Kulozik, 2021), which likely caused it to assemble differently at the oil-water interface than the protease inhibitor-rich Potato-2.

It is clearly difficult to establish a link between surface rheological parameters determined in small amplitude shear or dilatational deformations, and dynamic stability of emulsions under flow. Instead, the rheological response in the LVE and NLVE is needed to assess this stability, and that is still rarely done for plant-protein isolate stabilised interfaces. These results are helpful to evaluate the effects of surface parameters on dynamic emulsion stability under processing conditions, as they may, for example, occur in the processing of plant-based dairy drinks. The results may also have ramifications for the processing of other types of products, such as plant-based meat replacers. These are often produced using extrusion, and in that process emulsion droplets dispersed in the protein matrix to control juiciness, are also subjected to high shear and extensional strains. Our findings can help in the selection of suitable stabilisers to stabilise emulsions in such dynamic conditions. Although care must be taken to extrapolate our results to actual extrusion processes. Stresses applied to the interfaces by a dense protein matrix which is extruded through a die of an extruder, can be significantly higher than the shear forces we applied here using an Ultra Turrax.

CRediT authorship contribution statement

Naoya Ikenaga: Investigation, Formal analysis, Validation, Writing – Original Draft. Leonard M.C. Sagis: Conceptualisation, Methodology, Writing – Review & Editing, Supervision, Project administration.

Declaration of competing interest

The authors declare that no competing interests exist.

Data availability

Data will be made available on request.

Acknowledgement

This research is part of the project PlantPROMISE, which is co-financed by Top Consortium for Knowledge and Innovation Agri & Food by the Dutch Ministry of Economic Affairs; The project is registered under contract number LWV-19027.

Appendix A. Supplementary data

Supplementary data to this article can be found online at https://doi.org/10.1016/j.foodhyd.2023.109248.

References

Akharume, F. U., Aluko, R. E., & Adedeji, A. A. (2021). Modification of plant proteins for improved functionality: A review. *Comprehensive Reviews in Food Science and Food Safety, 20*(1), 198–224.

Andlinger, D. J., Röscheisen, P., Hengst, C., & Kulozik, U. (2021). Influence of pH, temperature and protease inhibitors on kinetics and mechanism of thermally induced aggregation of potato proteins. *Foods, 10*(4), 796.

Arunkumar, N., Deecaraman, M., & Rani, C. (2009). Nanosuspension technology and its applications in drug delivery. *Asian Journal of Pharmaceutics, 3*(3).

Braun, K., Hanewald, A., & Vilgis, T. A. (2019). Milk emulsions: Structure and stability. *Foods, 8*(10), 483.

Cicuta, P., Stancik, E. J., & Fuller, G. G. (2003). Shearing or compressing a soft glass in 2D: Time-concentration superposition. *Physical Review Letters, 90*(23), Article 236101.

Cornet, S. H., Snel, S. J., Schreuders, F. K., van der Sman, R. G., Beyrer, M., & van der Goot, A. J. (2022). Thermo-mechanical processing of plant proteins using shear cell and high-moisture extrusion cooking. *Critical Reviews in Food Science and Nutrition, 62*(12), 3264–3280.

Delgado, M., Lázaro, A., Biedenbach, M., Gamisch, S., Gschwander, S., Höhlein, S., et al. (2018). Intercomparative tests on viscosity measurements of phase change materials. *Thermochimica Acta, 668*, 159–168.

Donley, G. J., Singh, P. K., Shetty, A., & Rogers, S. A. (2020). Elucidating the G″overshoot in soft materials with a yield transition via a time-resolved experimental strain decomposition. *Proceedings of the National Academy of Sciences, 117*(36), 21945–21952.

Erni, P., Windhab, E. J., Gunde, R., Graber, M., Pfister, B., Parker, A., et al. (2007). Interfacial rheology of surface-active biopolymers: Acacia Senegal gum versus hydrophobically modifed starch. *Biomacromolecules, 8*(11), 3458–3466.

Ewoldt, R. H., Hosoi, A. E., & Mckinley, G. H. (2008). New measures for characterizing nonlinear viscoelasticity in large amplitude oscillatory shear. *Journal of Rheology, 52*(6), 1427–1458.

Ewoldt, R. H., Johnston, M. T., & Caretta, L. M. (2015). Experimental challenges of shear rheology: How to avoid bad data. In S. Spagnolie (Ed.), *Complex fluids in biological systems. Biological and medical physics, biomedical engineering* (pp. 207–241). Springer.

Fardin, M. A., Perge, C., Casanellas, L., Hollis, T., Taberlet, N., Ortín, J., et al. (2014). Flow instabilities in large amplitude oscillatory shear: A cautionary tale. *Rheologica Acta, 53*(12), 885–898.

Felix, M., Yang, J., Guerrero, A., & Sagis, L. M. (2019). Effect of cinnamaldehyde on interfacial rheological properties of proteins adsorbed at O/W interfaces. *Food Hydrocolloids, 97*, Article 105235.

García-Moreno, P. J., Yang, J., Gregersen, S., Jones, N. C., Berton-Carabin, C. C., Sagis, L. M., et al. (2021). The structure, viscoelasticity and charge of potato peptides adsorbed at the oil-water interface determine the physicochemical stability of fish oil-in-water emulsions. *Food Hydrocolloids, 115*, Article 106605.

Hinderink, E. B. A., Sagis, L., Schroën, K., & Berton-Carabin, C. C. (2020). Behavior of plant-dairy protein blends at air-water and oil-water interfaces. *Colloids and Surfaces B: Biointerfaces, 192*, Article 111015.

Hinderink, E. B., Sagis, L., Schroën, K., & Berton-Carabin, C. C. (2021). Sequential adsorption and interfacial displacement in emulsions stabilized with plant-dairy protein blends. *Journal of Colloid and Interface Science, 583*, 704–713.

Hong, J. S., Kong, H. J., Hyun, K., Bergfreund, J., Fischer, P., & Ahn, K. H. (2019). Rheological analysis of oil–water emulsions stabilized with clay particles by Laos and interfacial shear moduli measurements. *Rheologica Acta, 58*(8), 453–466.

Hyun, K., Kim, S. H., Ahn, K. H., & Lee, S. J. (2002). Large amplitude oscillatory shear as a way to classify the complex fluids. *Journal of Non-Newtonian Fluid Mechanics, 107*(1–3), 51–65.

Jaishankar, A., & McKinley, G. H. (2013). Power-law rheology in the bulk and at the interface: Quasi-properties and fractional constitutive equations. *Proceedings of the Royal Society A: Mathematical, Physical and Engineering Sciences, 469*(2149), Article 20120284.

Kendler, C., Duchardt, A., Karbstein, H. P., & Emin, M. A. (2021). Effect of oil content and oil addition point on the extrusion processing of wheat gluten-based meat analogues. *Foods, 10*(4), 697.

Kieserling, H., Alsmeier, I. M., Steffen-Heins, A., Keppler, J. K., Sevenich, R., Rauh, C., et al. (2021). Interfacial film formation and film stability of high hydrostatic pressure-treated β-lactoglobulin. *Food Hydrocolloids, 119*, Article 106746.
Läuger, J., & Stettin, H. (2016). Effects of instrument and fluid inertia in oscillatory shear in rotational rheometers. *Journal of Rheology, 60*(3), 393–406.
Liang, H.-N., & Tang, C.-h. (2014). Pea protein exhibits a novel Pickering stabilization for oil-in-water emulsions at pH 3.0. *LWT-Food Science & Technology, 58*(2), 463–469.
Liu, C., Bhattarai, M., Mikkonen, K. S., & Heinonen, M. (2019). Effects of enzymatic hydrolysis of fava bean protein isolate by alcalase on the physical and oxidative stability of oil-in-water emulsions. *Journal of Agricultural and Food Chemistry, 67*(23), 6625–6632.
Lucassen, J., & Van Den Tempel, M. (1972). Dynamic measurements of dilational properties of a liquid interface. *Chemical Engineering Science, 27*(6), 1283–1291.
Mäkinen, O. E., Wanhalinna, V., Zannini, E., & Arendt, E. K. (2016). Foods for special dietary needs: Non-dairy plant-based milk substitutes and fermented dairy-type products. *Critical Reviews in Food Science and Nutrition, 56*(3), 339–349.
Mariotti, F., Tomé, D., & Mirand, P. P. (2008). Converting nitrogen into protein—beyond 6.25 and Jones' factors. *Critical Reviews in Food Science and Nutrition, 48*(2), 177–184.
McClements, D. J., Lu, J., & Grossmann, L. (2022). Proposed methods for testing and comparing the emulsifying properties of proteins from animal, plant, and alternative sources. *Colloids and Interfaces, 6*(2), 19.
Mefleh, M., Pasqualone, A., Caponio, F., & Faccia, M. (2022). Legumes as basic ingredients in the production of dairy-free cheese alternatives: A review. *Journal of the Science of Food and Agriculture, 102*(1), 8–18.
Munekata, P. E., Domínguez, R., Budaraju, S., Roselló-Soto, E., Barba, F. J., Mallikarjunan, K., et al. (2020). Effect of innovative food processing technologies on the physicochemical and nutritional properties and quality of non-dairy plant-based beverages. *Foods, 9*(3), 288.
Ntone, E., Van Wesel, T., Sagis, L. M. C., Meinders, M., Bitter, J. H., & Nikiforidis, C. V. (2021). Adsorption of rapeseed proteins at oil/water interfaces. Janus-like napins dominate the interface. *Journal of Colloid and Interface Science, 583*, 459–469.
Osen, R., Toelstede, S., Wild, F., Eisner, P., & Schweiggert-Weisz, U. (2014). High moisture extrusion cooking of pea protein isolates: Raw material characteristics, extruder responses, and texture properties. *Journal of Food Engineering, 127*, 67–74.
Phianmongkhol, A., & Varley, J. (2003). ζ potential measurement for air bubbles in protein solutions. *Journal of Colloid and Interface Science, 260*(2), 332–338.
Riddick, T. M. (1968). *Control of stability through zeta potential*. New York: Zeta Meter Inc.
Rühs, P. A., Scheuble, N., Windhab, E. J., & Fischer, P. (2013). Protein adsorption and interfacial rheology interfering in dilatational experiment. *The European Physical Journal - Special Topics, 222*(1), 47–60.
Sagis, L. M., & Fischer, P. (2014). Nonlinear rheology of complex fluid–fluid interfaces. *Current Opinion in Colloid & Interface Science, 19*(6), 520–529.
Schramm, L. L. (2005). *Emulsions, foams, and suspensions fundamentals and applications*. Weinheim: Wiley-VCH Verlag.
Singh, M., Trivedi, N., Enamala, M. K., Kuppam, C., Parikh, P., Nikolova, M. P., et al. (2021). Plant-based meat analogue (PBMA) as a sustainable food: A concise review. *European Food Research and Technology, 247*(10), 2499–2526.
Sridharan, S., Meinders, M. B., Bitter, J. H., & Nikiforidis, C. V. (2020). Pea flour as stabilizer of oil-in-water emulsions: Protein purification unnecessary. *Food Hydrocolloids, 101*, Article 105533.
Tan, Y., Wannasin, D., & McClements, D. J. (2022). *Utilization of potato protein fractions to form oil-in-water nanoemulsions: Impact of pH, salt, and heat on their stability*. Food Hydrocolloids, Article 108356.
Wang, H., Zhang, L., Czaja, T. P., Bakalis, S., Zhang, W., & Lametsch, R. (2022). Structural characteristics of high-moisture extrudates with oil-in-water emulsions. *Food Research International, 158*, Article 111554.
Winter, H. H., & Mours, M. (1997). Rheology of polymers near liquid-solid transitions. In *, Vol. 134. Neutron spin echo spectroscopy viscoelasticity rheology. Advances in polymer science* (pp. 165–234). Berlin, Heidelberg: Springer.
Yang, J., de Wit, A., Diedericks, C. F., Venema, P., van der Linden, E., & Sagis, L. M. (2021). Foaming and emulsifying properties of extensively and mildly extracted Bambara groundnut proteins: A comparison of legumin, vicilin and albumin protein. *Food Hydrocolloids, 123*, Article 107190.
Yang, J., Faber, I., Berton-Carabin, C. C., Nikiforidis, C. V., Van Der Linden, E., & Sagis, L. M. C. (2021). Foams and air-water interfaces stabilised by mildly purified rapeseed proteins after defatting. *Food Hydrocolloids, 112*, Article 106270.
Yang, J., Thielen, I., Berton-Carabin, C. C., van der Linden, E., & Sagis, L. M. (2020). Nonlinear interfacial rheology and atomic force microscopy of air-water interfaces stabilized by whey protein beads and their constituents. *Food Hydrocolloids, 101*, Article 105466.
Yang, J., Waardenburg, L. C., Berton-Carabin, C. C., Nikiforidis, C. V., van der Linden, E., & Sagis, L. M. (2021). Air-water interfacial behaviour of whey protein and rapeseed oleosome mixtures. *Journal of Colloid and Interface Science, 602*, 207–221.
Zhang, J., Liu, L., Jiang, Y., Faisal, S., & Wang, Q. (2020). A new insight into the high-moisture extrusion process of peanut protein: From the aspect of the orders and amount of energy input. *Journal of Food Engineering, 264*, Article 109668.
Zhou, X., Sala, G., & Sagis, L. M. (2020). Bulk and interfacial properties of milk fat emulsions stabilized by whey protein isolate and whey protein aggregates. *Food Hydrocolloids, 109*, Article 106100.